

# Measurements of the Modulation Transfer Function of Image Displays

S. Triantaphillidou and R. E. Jacobson<sup>▲</sup>

*Imaging Technology Research Group, University of Westminster, School of Media, Arts and Design, Harrow Campus, Harrow, United Kingdom*

Measurements of the Modulation Transfer Function (MTF) of image displays are often required for objective image quality assessments, but are difficult to carry out due to the need for specialized apparatus. This article presents a simple method for the measurement of the MTF of a sample CRT display system which involves the use of a still digital camera for the acquisition of displayed test targets. Measurements are carried out using, first, the sine wave method, where a number of artificial sine wave images of discrete spatial frequency and constant modulation are captured from a close distance. Fourier techniques are employed to extract the amplitude of the display signal from the resulting macroimages. In a second phase, displayed artificial step edges are captured, and the ISO 12333 SFR (Spatial Frequency Response) Slanted Edge plug-in is used for automatic edge analysis. The display MTF, in both cases, is cascaded from the closed-loop system MTF. The two measuring techniques produced matching results, indicating that under controlled test conditions accurate measurements of the display MTF can be achieved with the use of relatively simple equipment.

Journal of Imaging Science and Technology 48: 58–65 (2004)

## Introduction

While the tone and color reproduction of image displays have been widely explored in the last two decades<sup>1–5</sup> and can be measured with relatively inexpensive equipment, measurements of the modulation transfer function (MTF) of displays are rarely described. This can be attributed partially to the need for expensive, specialized apparatus necessary to carry out the task. MTF evaluation of image displays is nevertheless very often needed in the assessment of objective image quality, especially in the application of image quality metrics.<sup>6,7</sup> In this work, the monochrome MTF of a modern cathode ray tube (CRT) display system was determined by employing a still digital camera of medium resolution. The work demonstrates and compares two MTF measuring techniques (the *sine wave* and the *slanted edge*) for the evaluation of the display MTF, using the camera as the measuring device and a CRT display as a model system.

The camera system consisted of the Kodak DCS420m monochrome digital camera, which at its nominal speed of ISO 200 operates with minimal image processing<sup>8</sup> and the Twain 3.2 driving software with all optional image processing parameters turned off. The MTF was evaluated for the horizontal and vertical display orientations, of the central display area.

## The Display System

The display system consisted of a 17 inch NEC MultiSync P750 Cromaclear CRT.<sup>9,10</sup> It was driven by a

Matrox Graphics MGA Millennium graphics card in the host IBM-compatible personal computer. The mask pitch of the NEC P750 is 0.25 mm, aligned in a slot mask arrangement. When combined with the slot mask the red, green and blue P-22 phosphors of the CRT appear elliptical in shape, compared to round phosphors used in trio dot CRTs and stripes used in aperture grille systems. The illuminated phosphors are also grouped in separate bundles of three in a vertical alignment (see Fig. 1). The graphics card was configured to display 8 bits per channel at an addressable resolution of 1024 by 768 pixels and a refresh frequency of 75 Hz.

All display measurements were carried out in a darkened laboratory. The display set-up was carried out in a similar fashion to that described by Ford,<sup>11</sup> producing a calibrated white point close to  $D_{65}$  and aiming to achieve

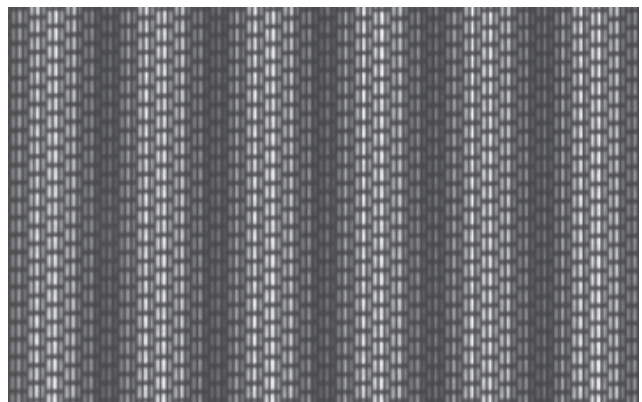


**Figure 1.** A captured sine wave target displayed on the CRT.

Original manuscript received January 28, 2003

▲ IS&T Member

©2004, IS&T—The Society for Imaging Science and Technology

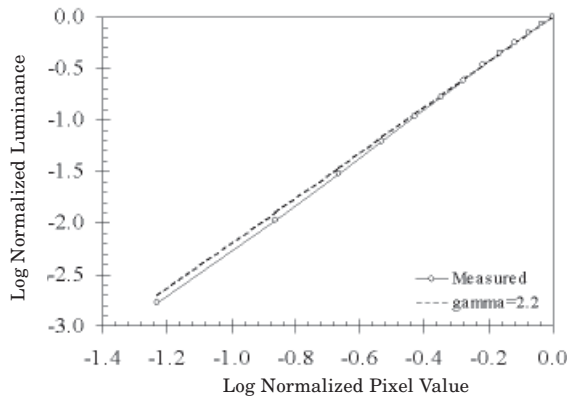


Figure 2. The display transfer function.

the maximum contrast range, with the darkest possible black point and no loss in the available intensity levels. Optimization of the focus was performed in the central area of the faceplate. After adjustments the displayed image occupied an area of 306 mm horizontally and 230 mm vertically on the CRT faceplate. The physical dimensions of the active display area and the addressable resolution of the graphics card yielded an average pixel size of 0.299 mm by 0.299 mm, i.e., approximately 1.20 phosphor bundles per pixel. The calculated horizontal and vertical resolution was 3.34 pixels/mm and the theoretical Nyquist frequency 1.67 cycles/mm.

The monochrome transfer function of the display system was determined by measuring fourteen monochrome patches, one at a time, ranging from the system black to the maximum white. A custom made application developed in C++ was employed to display each patch in the central (proportional to the faceplate) rectangle occupying 50% of the faceplate, with the surrounding area displaying the inverse intensity to ensure equal loading of the system at all measured levels.<sup>12</sup> The resulting transfer function fits closely to the transfer function of the sRGB reference display system,<sup>13</sup> which is typical for correctly adjusted CRTs. It is illustrated in  $\log_{10}$ - $\log_{10}$  space in Fig. 2. Finally, linear interpolation in  $\log_{10}$ - $\log_{10}$  space was applied to the measured data to develop a look-up table (LUT) that was used in later stages for the necessary linearization of the display signal.

### The Camera System

The DCS420m digital camera operates with a conventional 35 mm single lens reflex camera body and a CCD area array of 1524 by 1012 photoelements with approximately 9.1  $\mu\text{m}$  pitch.<sup>14</sup> The Nyquist limit of the CCD array is 55 cycles/mm and its physical size 13.8 by 9.2 mm, with 3:2 aspect ratio. The fill factor is not specified but a typical value for this type of digital cameras is near 90%.<sup>15</sup> The camera acquires images at 12 bits tonal resolution. The output signal is transfer corrected and down-sampled to 8 bits for output, resulting in 1.5 MB digital image files. The files are stored on a PCMCIA-ATA standard memory card in the camera, as TIFF uncompressed 8 bit images. The camera body was equipped with an auto-focus Macro Nikkor 60 mm f/2.8D lens. The effective focal length of the lens with the size of the camera's imaging sensor is 2.6 times the quoted focal length, i.e., approximately 156 mm.<sup>14</sup> A Tiffen infra-red absorbing filter was mounted on the lens to re-

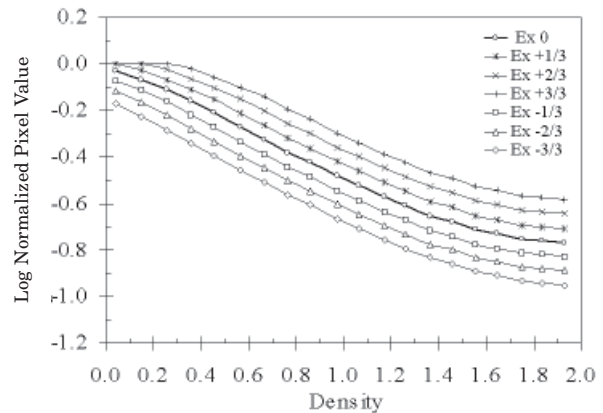


Figure 3. Camera transfer functions for seven different exposures.

duce near infra-red absorption, resulting in less noisy digital images and better lens MTF performance.<sup>16</sup>

The camera/lens system was rigidly mounted on a tripod, with its optical axis being orthogonal to the plane of the target and operated in self-timer mode to minimize distortions caused by camera shake. Only the central 50% of the capturing frame was used in the measurements, to reduce distortions within the recording area introduced by any array spatial inconsistencies,<sup>17</sup> lens variations,<sup>18</sup> uneven lighting, etc. Automatic spot focusing, providing optimum focus in the central area of the frame and increased consistency over manual focus. Manual exposure spot meter modes were employed in the recording of the data, unless stated otherwise. The lens was always set to aperture priority mode and operated with apertures of either f/11 or f/8. The same camera, lens and filter, driving software and settings were used throughout this work. Accordingly, the performances of all the components of the acquisition system were evaluated in combination.

The tone reproduction of the DCS420m was evaluated for different camera exposures, ranging from -1 to +1 stops, at 1/3 of a stop intervals. This was achieved by capturing a Kodak Q-13 20-step grayscale mounted on a Kodak R-27 18% graycard and illuminated by two Photoflood 200W tungsten lamps. Correct exposure here, as for every reflection target photographed in later stages, was determined from a Kodak R-27 graycard and from the central part of the frame, using the through-the-lens built-in spot meter of the camera. Even illumination within the capturing frame, i.e., within 1/3 of a stop, was assured by measuring 12 approximately equally spaced points (4  $\times$  3) covering the entire imaging area. Five images of the target were recorded, each with a slight displacement of the grayscale within the imaging frame. The measured transfer functions of the camera (average data from five frames) for seven different exposures are illustrated, in  $\log_{10}$ - $\log_{10}$  space, in Fig. 3.

### MTF Measurements

It is widely known that the determination of the MTF of imaging systems often depends on the measuring technique due to nonlinearities the systems introduce.<sup>19,20</sup> The MTF of the display system and that of the acquisition system were evaluated using two different techniques: the sine wave method and the ISO 12233 Slanted Edge method.<sup>21</sup> Although the term SFR is used instead of MTF in the official title of the standard to avoid con-

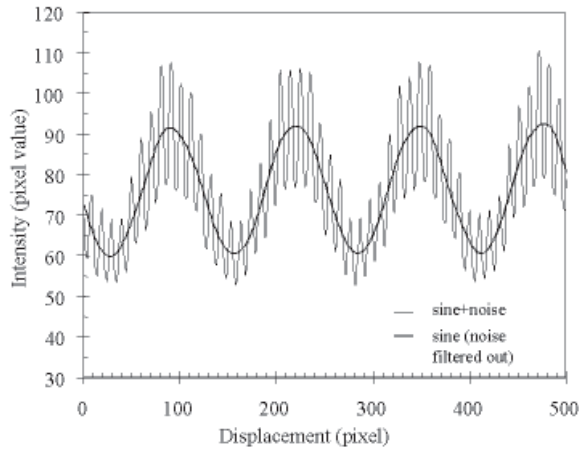


Figure 4. The averaged output signal in real space.

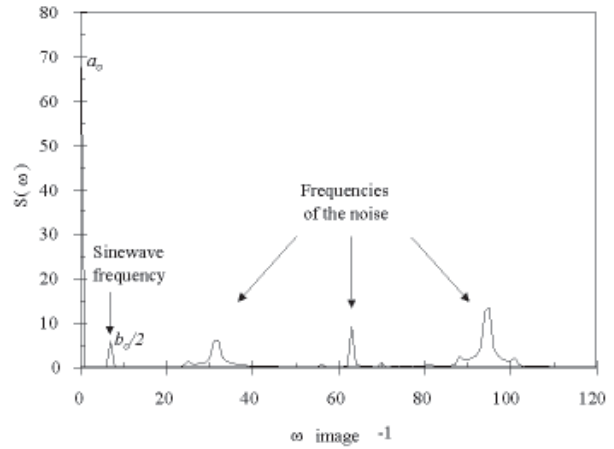


Figure 5. The averaged output signal in Fourier space.

fusion with photographic MTF,<sup>22</sup> in this work we refer to the result obtained from the ISO calculations as SFR and to that excluding the frequency content of the test target as MTF. The display MTF was obtained, each time, by removing the MTF of the acquisition system from the closed-loop system MTF.

### The Sine Wave Method

The principles of the sine wave method for MTF evaluation of imaging systems are described by Dainty et al.<sup>23</sup> For display measurements, this method involved the display of artificial test images, 256 pixels square, with one-dimensional sinusoidal varying intensity, generated by:

$$I(x) = a + b \sin(\pi\omega x) \quad (1)$$

where  $I(x)$  denotes the generated pixel value at an horizontal displacement from the origin of pixels  $x$ ,  $a$  the average signal level,  $b$  the signal amplitude and  $\omega$  the spatial frequency.  $b/a$  gives the modulation of the input signal. Sine wave targets of twelve discrete spatial frequencies ranging from 0.04 to 0.50 cycles per pixel were used, with two different modulations 0.20 and 0.50 at a mean pixel value of 128.

Each sinusoidal test target was displayed, one at a time, in the center of the CRT faceplate with the remaining of the active display area set to 18% of the peak luminance. The display functions of Matlab image processing software were used for the purpose. The targets were displayed in two orientations, at right angle to each other, to evaluate the frequency responses of the horizontal and the vertical display orientations. The camera was placed very close to the CRT faceplate, with its optical axis exactly orthogonal and centered on the faceplate within one display pixel precision. This precision was necessary for the later analysis of the recorded data. The camera lens was covered with a black hood to reduce flare and was set to an aperture of  $f/11$ , which provided an increased depth of field covering the slight curvature of the CRT faceplate. Correct exposure was identified by photographing a slightly defocused (to blur the grid and phosphor structure) gray patch with luminance 18% of the peak white. Spatial calibration was achieved by photographing a millimeter scale, fabricated on card and placed in contact with the center of the CRT faceplate.

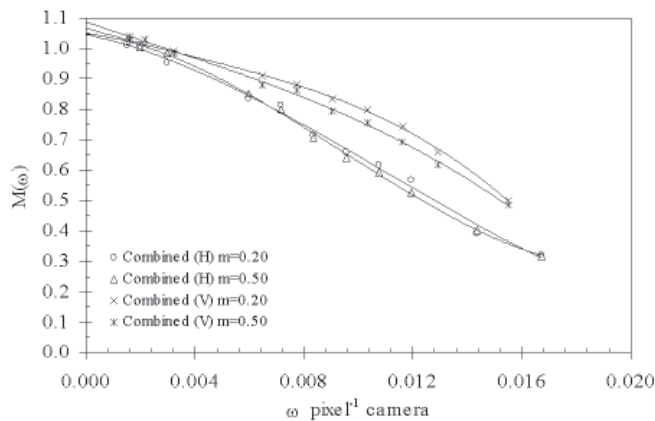
Five successive frames were captured for each target and at each target orientation, to allow average results

with reduced noise in the temporal dimension caused by mismatch between screen refresh rate and camera synchronization. To avoid data clipping and place the image data in the central part of the camera transfer function, targets with modulation 0.20 were underexposed by 1/3 of a stop, whereas 2/3 of a stop underexposure was used to capture targets with modulation 0.50. Images were inspected for correct focus and accurate display-camera alignment before they were saved on the hard disk of the host computer as TIFF uncompressed files. For the horizontal display orientation, the camera captured 17.15 mm of the CRT faceplate. This gave a resolution of 26.6 camera pixels per CRT pixel. On the other hand, for the vertical display orientation, the camera was placed slightly further from the CRT and captured a distance of 18.59 mm on the faceplate. This gave a resolution of 24.6 camera pixels per CRT pixel.

### Combined Camera-Display MTF

The acquired digital images were processed using custom made routines in the Matlab environment as follows: Mean pixel values perpendicular to the direction of propagation were obtained. In this way, display noise effects and luminance inhomogeneity resulting from the phosphor persistency characteristics<sup>24</sup> were minimized in a similar way to integrating with a thin long slit.<sup>25</sup> Careful alignment of the camera as well as the high magnification allowed this simulation without introducing errors, even at high spatial frequencies. The resulting one-dimensional traces were then converted into linear luminance units using a LUT representing the combined transfer function of the acquisition and the display system.

Figure 4 presents an example of a one-dimensional trace in real space. The large amplitude fluctuations relative to the sine wave signal at the input frequency are due to the shadow mask arrangement, which is resolved when the screen is photographed at such a high magnification. In Fourier space, this non-linear noise was identified as a set of peaks at discrete frequencies, beyond the Nyquist frequency of the display (see Fig. 5). Half the amplitude of the output sine wave,  $b_o/2$ , and the mean signal level,  $a_o$ , were also available and were extracted from the Fourier domain at the corresponding sine wave frequency and the zero frequency respectively. Figure 5 illustrates an example of the sine wave trace in Fourier space, with frequency at 7 cycles per



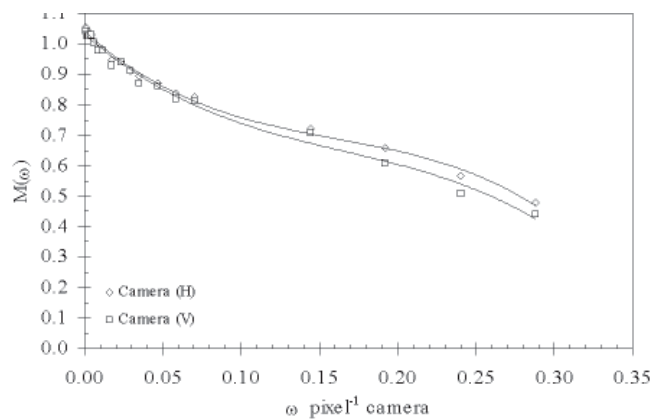
**Figure 6.** MTF curves for the horizontal (H) and vertical (V) display-camera orientations for two input modulations ( $m$ ), determined with sine waves.

image. It is worth noting that because of the nature of the discrete Fourier transform: i) entire cycles, or multiples of them, have to be transformed to extract the accurate  $b_o/2$  at the correct spatial frequency; ii) the resulting  $b_o/2$  and  $a_o$  need to be re-scaled, i.e., divided by the length of the trace, which is the scaling factor in Matlab. The output (display-camera) modulation was evaluated for each spatial frequency from  $b_o/a_o$ , and the MTF was determined from the ratio of output to input modulation. Measurement accuracy decreases with increased sine wave frequency owing to phase and noise problems.<sup>20</sup> During this work, measurements were limited to 0.44 and 0.38 cycles per CRT pixel, i.e., 88% and 76% of the Nyquist frequency, for the horizontal and vertical display orientations respectively.

Figure 6 illustrates the horizontal and vertical MTF curves of the combined camera-display system as a function of cycles per camera pixel for two input modulations. The points in the figure represent the measured data and the continuous lines third degree polynomial functions which successfully fitted the data. Third degree polynomial functions as well as exponential functions (often used to fit the display MTF<sup>11</sup>) represented with equal success the combined system MTF.

### Camera MTF

Measurements of the MTF of the acquisition system were carried out using a commercially calibrated reflection target,<sup>26</sup> including fifteen sinusoidal patches of known spatial frequency and average modulation of 0.60. Target illumination, camera exposure and spatial calibration were organized in a similar fashion to that described earlier. Each patch on the target was photographed separately, at both horizontal and vertical directions of sine wave propagation, to evaluate the MTF for both horizontal, i.e., landscape, and vertical, i.e., portrait, camera orientations. Some patches were photographed twice from different distances so that, in the end, nineteen different spatial frequencies covering a range from approximately 0.001 to 0.30 cycles per camera pixel contributed to the measured MTF. Multiple one-dimensional sinusoidal traces were extracted from each patch and were converted to linear reflectance units by employing the appropriate transfer LUT for the acquisition system. The methodology for extracting the modulation in discrete systems has been described earlier.<sup>20</sup> Phase and noise problems encountered in the measurements at high spatial frequencies were not sig-



**Figure 7.** MTF curves for the horizontal (H) and vertical (V) camera orientations, determined with sine waves.

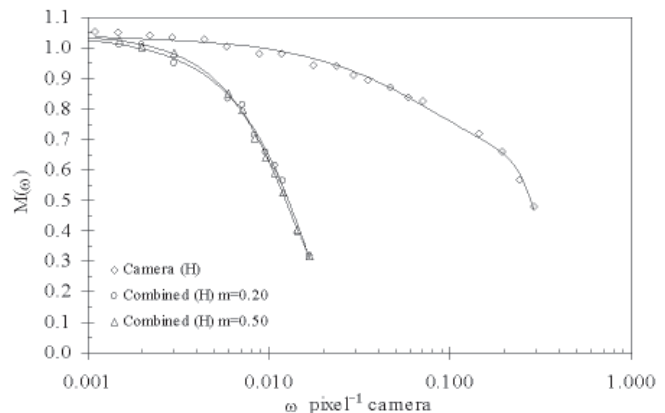


**Figure 8.** MTF curves for the horizontal (H) display-camera orientation and the MTF of the horizontal camera orientation alone, determined with sine waves.

nificant, since only lower spatial frequencies (relative to the camera's sampling frequency) were of interest for cascading the display MTF. MTF curves for both horizontal and vertical camera orientations up to 60% of the Nyquist limit of the device are shown in Fig. 7. Figure 8 illustrates MTF curves of the combined display-camera system and the camera system alone, for the horizontal display and camera orientations. It is noticed that due to the high magnification used to capture the displayed test targets, the spatial frequencies of interest for cascading the display MTF are relatively low (up to  $\approx 0.020$  pixel<sup>-1</sup>). Over this range of frequencies the response of the camera is almost constant.

### Display MTF

The MTF of the display system was finally cascaded by dividing the combined system MTF by that of the camera system. For this it was assumed that each component was linear and that the MTF for each successive component was independent from that of the previous component.<sup>27</sup> MTF curves of the display system determined with this method are illustrated in Fig. 9. The outcomes obtained with this method suggest that once the output signal is corrected for nonlinearities, the frequency responses of the system are relatively independent from the input modulation. This is a surprising result when considering the strong dependence

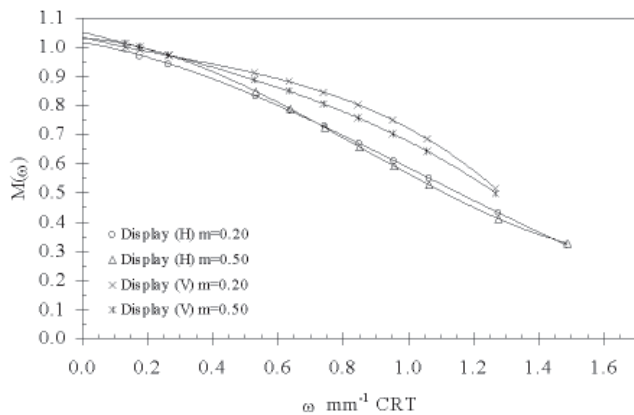


**Figure 9.** MTF curves for both display orientations and two input modulations, determined with sine waves.

of the CRT performance on the levels of display luminance. Horizontal and vertical MTFs differ, but not considerably (especially when the variations in the measurements are taken into account; see Fig. 10) with the vertical system response being slightly higher at increased spatial frequencies. The limit of the resolvable frequencies is higher for the horizontal than for the vertical display orientations. Both effects are due to the interaction between addressed pixels, phosphor groups, the shadow mask, and the raster scan of the CRT, which varies with orientation. An estimate of the error, indicating the inaccuracy in the measured MTFs, was obtained by measuring the variation of the output modulation.

### ISO 12233 Slanted Edge Method

The ISO 12233<sup>21</sup> Spatial Frequency Response (SFR) plug-in (for Adobe Photoshop software) was developed

to determine the SFR of digital cameras from images of sloping edges. For display measurements this method involved the display of artificial step edges with two different modulations of 0.50 and 0.70. The edges were generated in Matlab and displayed in a similar way to the sine wave targets. Edges with lower modulation did not produce the necessary contrast for the SFR plug-in to operate appropriately.<sup>29</sup> The camera was placed approximately 80 cm from the CRT covering a distance of 178.2 mm on the faceplate. The camera distance warranted that more than two camera pixels, i.e., 2.6 camera pixels, were dedicated per display pixel, whereas it allowed the necessary blending so that the noise introduced by the phosphor and mask arrangement would not prevent the plug-in operations. Correct exposure and spatial calibration were carried out as described earlier. The edges were captured with a slope of approximately 15° from the vertical.<sup>30</sup> This was achieved by tilting the camera while its optical axis remained orthogonal to the CRT faceplate. Five consecutive frames were captured for each target, with the edge translated slightly at each shot within an area of 20 mm square on the faceplate to obtain average results. The process was carried out for both horizontal and vertical display orientations.

### Combined Camera-Display MTF

A third degree polynomial fitted successfully the combined camera-display transfer function, to develop a 256 step LUT that served as the Opto-Electronic Conversion Function (OECF), necessary for the linearization of the data during the plug-in operations.<sup>29</sup> A rectangular region-of-interest (ROI) covering 46 by 280 pixels (with respect to the measuring orientation) was selected from each frame, over which the calculations of the plug-in were carried out. The vertical to horizontal aspect ratio of the ROI was kept as high as possible to increase the signal-to-noise ratio of the SFR estimates.<sup>30</sup> The measurements covered approximately the same display area to that covered during the sine wave measure-

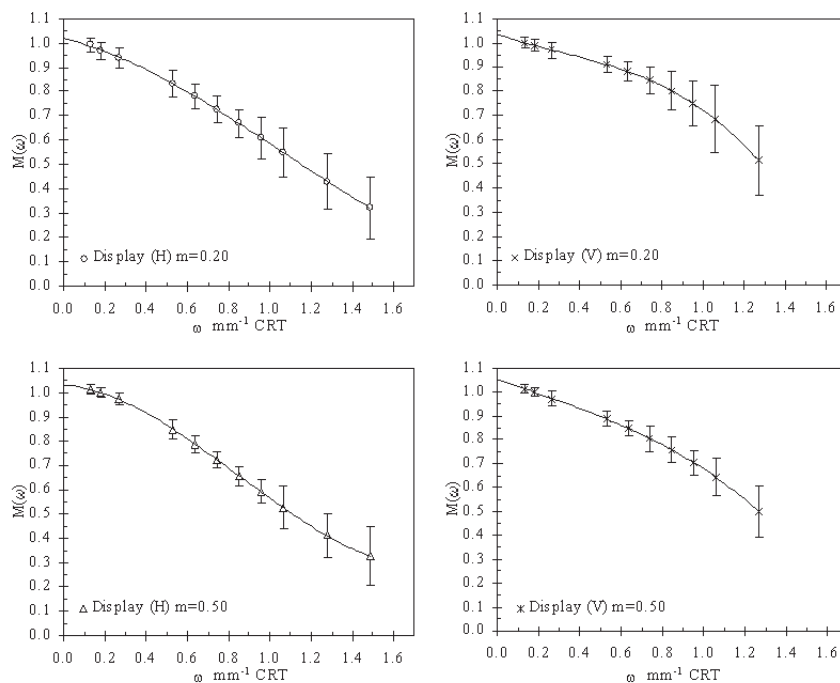


**Figure 10.** Display MTF curves determined with sine waves, including the measurement error.

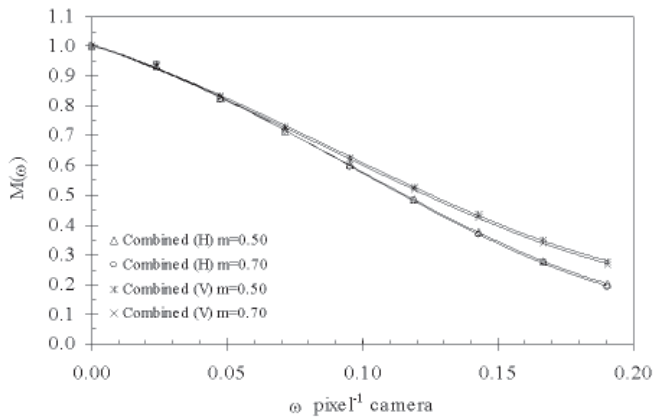


**Figure 11.** MTF curves for the horizontal (H) and vertical (V) display-camera orientations for two input modulations ( $m$ ), determined with the ISO 12233.

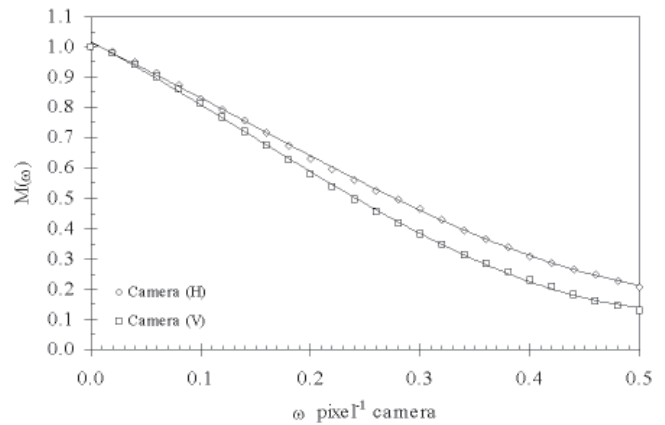


**Figure 12.** MTF curves for the horizontal (H) and vertical (V) camera orientations, determined with the ISO 12233.

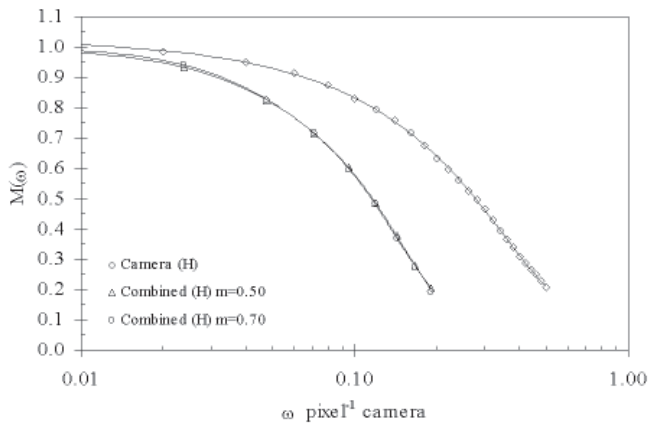


**Figure 13.** MTF curves for the horizontal (H) display-camera orientation and the MTF of the horizontal camera orientation alone, determined with the ISO 12233.

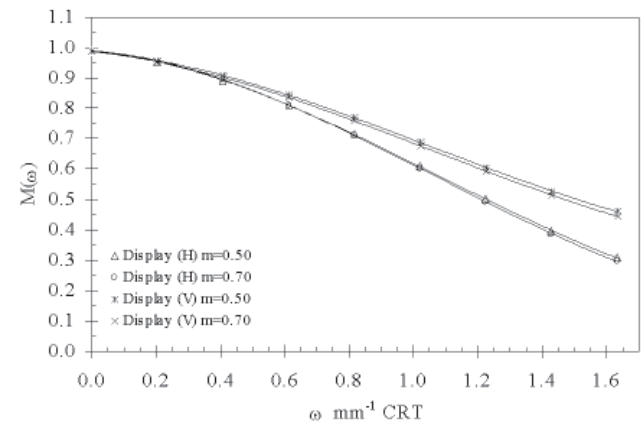


**Figure 14.** MTF curves for both display orientations and two input modulations, determined with the ISO 12233.

ments. Average frequency responses were calculated for each target and each target orientation; third degree polynomial functions fitted the measured data. The frequency response of the combined camera-display system and are illustrated in Fig. 11.

### Camera MTF

The average frequency response of the acquisition system to an edge target was evaluated by photographing a high quality laser printed step edge, at a magnification of 0.05. The edge was printed as a binary digital image file, at 600 dpi. A number of density measurements were taken from the print to secure that the edge maintained uniform density along its length. The frequency content of the target was not measured. However, the very low magnification of the system allowed the reasonable assumption that it was constant over the spatial frequencies of interest.<sup>15</sup> Target illumination, exposure and spatial calibration were arranged in the same way as with the reflection sine wave targets. The edge was captured and processed in the same way as the displayed edges to evaluate the spatial frequency response for both horizontal and vertical camera orientations. Results are illustrated in Fig. 12, where the responses of the system are shown up to its Nyquist limit. Figure 13 presents the frequency responses of the combined system and of the camera system alone for

one display and camera orientation. The evaluation of the frequency response of the camera using this method gave results compatible with those obtained using the sine wave method. The spatial frequencies of interest for cascading the display MTF were up to approximately 0.20 pixel<sup>-1</sup>.

### Display MTF

The MTF of the display was extracted from the combined MTF. It is presented as a function of cycles/mm on the faceplate, for both input modulations, in Fig. 14. Similarly to the results obtained with the sine wave method, the MTF for the vertical display orientation was found to be higher than that for the horizontal orientation irrespective of the input modulation. The variation introduced in the display MTFs measured with the ISO technique (shown in Fig. 14 with error bars) was evaluated by calculating the  $M_{skew}(\omega)$  and  $M_{deri}(\omega)$  as explained by Burns.<sup>31</sup>

### Discussion

Figure 15 and 16 present MTF curves for both display orientations determined with the two measuring techniques. For the sine wave method, the curves are extrapolated to the theoretical Nyquist frequency of the display. With both techniques, neither MTF show significant differences. The sine wave method always gave

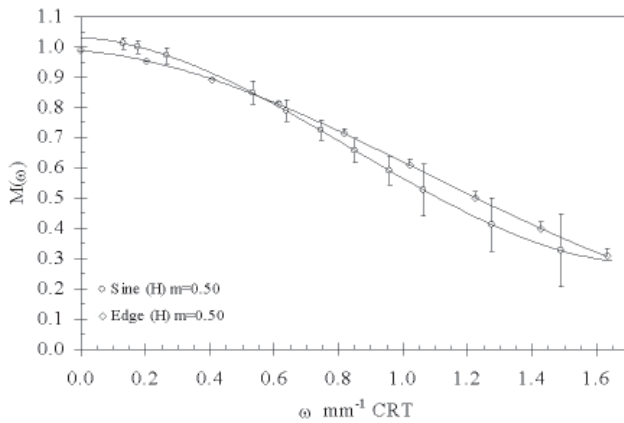


**Figure 15.** MTF curves for the horizontal (H) display orientation determined with the sine wave (sine) and the ISO 12233 (edge) methods.

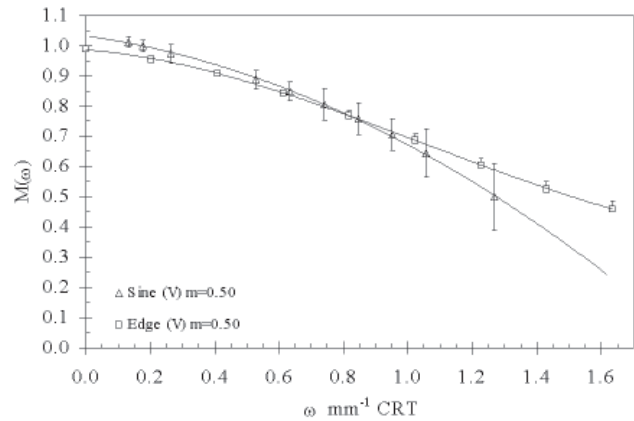


**Figure 16.** MTF curves for the vertical (V) display orientation determined with the sine wave (sine) and the ISO 12233 (edge) methods.

negligibly greater low frequency responses and poorer high frequency responses than the ISO 12233 method. The MTFs obtained with sine waves, however, were determined from the ratio of the absolute recorded modulation to the input modulation, i.e., the absolute contrast ratio was retained in the resulting MTF (see Eq. (2)), and rise slightly above unity at low spatial frequencies. This is in contrast with the MTFs determined with the ISO technique, which by default (and according to the mathematical definition of MTF) are normalized with respect to the zero frequency (DC) component. With both measuring techniques the horizontal display MTF was found slightly lower than the vertical MTF at middle and high spatial frequencies. The anisotropic behavior of the system is due to the raster nature of the CRT method of image formation, which varies with orientation, combined with the phosphor bundles and shadow mask arrangement. The produced display MTFs are similar to those obtained by Ford<sup>32</sup> measured with sine waves and with the aid of a low resolution video CCD camera and those evaluated by Feng et al.<sup>6</sup> who used the traditional edge method and a high resolution CCD sensor.

The sharpness of CRT displays in most cases is limited by the electro-optical focusing system or video bandwidth. For shadow-mask CRTs, spatial alignment, or convergence of the color components, have also a major impact on image sharpness. Generally, it is expected that, as a number of variables vary the MTF of the display will change. The system is not linear, therefore the MTF will also vary with average luminance level. Additionally, The response of the system at one point on the CRT is largely a function of the luminance of neighboring points and of the luminance of the background due to veiling glare effects.<sup>25</sup> Thus different backgrounds will produce varying results. Since CRTs are not isotropic, diagonal MTFs for the central display area should differ from the MTFs measured in this work. The MTF of the display is also expected to vary with spatial position, being higher at the central area where there is the shortest electron beam travel. Finally, since the composition of the red, green and blue phosphors differs, it is probable that the spatial frequency characteristics are different for each channel. MTF measurements of individual channels are nevertheless problematic, since it is hard to ensure that no secondary emissions result from a single channel input signal.<sup>2</sup>

## Conclusions

This study demonstrated a measuring technique for evaluating the display MTF that eliminates the need for expensive, specialized apparatus. It involved the use of a SLR monochrome digital camera for the acquisition of displayed test targets. The MTF of sample CRT display was determined using the sine wave and ISO 12233 measuring methods which yielded compatible results. Measurements were carried out only for a small central area of the faceplate, in the horizontal and vertical display orientations. With both techniques the amplitude of the horizontal display MTF was found slightly lower than that of the vertical MTF, with maximum discrepancies up to 0.2 occurring at increased spatial frequencies. Despite the fact that the characteristics of the CRT depend on the drive level, input modulations ranging from 0.20 to 0.70 produced similar spatial frequency responses. The measured MTFs can be considered as representative of the given system only for the given level of luminance, background luminance, display orientation and spatial location. ▲

## References

1. D. L. Post and C. S. Calhoun, An evaluation of methods for producing desired colors on CRT monitors, *Color Res. Appl.* **14**, 172 (1989).
2. R. S. Berns, R. J. Motta and M. E. Gorzynski, CRT colorimetry. part I: theory and practice, *Color Res. Appl.* **18**, 229 (1993).
3. R. S. Berns, R. J. Motta and M. E. Gorzynski, CRT colorimetry. part II: metrology, *Color Res. Appl.* **18**, 315 (1993).
4. L. Jimenez del Barco, J. A. Diaz, J. R. Jimenez and M. Rubino, Considerations on the calibration of color displays assuming constant channel chromaticity, *Color Res. Appl.* **20**, 377 (1995).
5. R. S. Berns, Methods for characterizing CRT displays, *Displays* **16**, 173 (1996).
6. Y. Feng, O. Östberg and B. Lindström, MTF as a measure for computer display screen image quality, *Displays* **11**, 186 (1990).
7. R. E. Jacobson, An evaluation of image quality metrics, *J. Photogr. Sci.* **43**, 7 (1995).
8. P. M. Hubel, Color image quality in digital cameras, *Proc. IS&T/PICS Conference*, IS&T, Springfield, VA, 1999, p. 153.
9. *NEC MultiSync P750 User's Manual*, NEC Europe Ltd., Germany (1997).
10. *Cromaclear CRT*, NEC Technologies, Internet publication: <http://www.necmitsubishi.com/products/home/cromaclear.cfm> (1999).
11. A. M. Ford, R. E. Jacobson and G. G. Attridge, Assessment of a CRT Display System, *J. Photogr. Sci.* **44**, 147 (1996).
12. D. Travis, *Effective Color Displays: Theory and Practice*, Academic Press, San Diego, 1991, pp. 154–160.
13. IEC 61966-2-1: Multimedia systems and equipment – Color measurement and management – Part 2-1: Color management – Default RGB color space – sRGB (1999).
14. *Kodak Professional DCS 420 Digital Camera – User's Manual*, Eastman Kodak Company, Part no. 692936, 1994.

15. R. B. Fagard-Jenkin, R. E. Jacobson and N. R. Axford, A novel approach to the derivation of expressions for geometrical MTF in sampled systems, *Proc. IS&T PICS Conference*, IS&T, Springfield, VA, 1999, p. 225.
16. R. B. Fagard-Jenkin, *Modulation transfer functions of digital acquisition devices*, PhD Thesis, University of Westminster, UK, 2001.
17. G. C. Holst, *CCD Arrays, Cameras and Display*, SPIE Optical Engineering Press, Bellingham, WA, 1996, ch. 3, p. 43–89.
18. S. Ray, *Applied Photographic Optics*, Focal Press, London, 1988, p. 217.
19. J. C. Dainty, Methods of measuring the modulation transfer function of photographic emulsions, *Opt. Acta*, **18**, 795 (1971).
20. S. Triantaphillidou, R. E. Jacobson and R. B. Fagard-Jenkin, An evaluation of MTF determination methods for 35 mm scanners, *Proc. IS&T PICS Conference*, IS&T, Springfield, VA, 1999, p. 231.
21. ISO 12233:2000, *Photography – Electronic picture camera – Resolution measurements*, International Standard Organization (2000).
22. ANSI PH 2.39-1977 (R1990), *Method of measuring the photographic modulation transfer function of continuous-tone, black-and-white photographic films*, American National Standards Institute, 1997.
23. J. C. Dainty and R. Shaw, *Image Science: Principles, Analysis and Evaluation of Photographic-Type Processes*, Academic Press, London, 1974, ch.7, p.232–275.
24. J. Peddie, *High-Resolution Graphics Display Systems*, Windcrest McGraw-Hill, New York, 1994, ch. 3., p. 107–188.
25. J. R. Banbury, Evaluation of MTF and veiling glare characteristics for CRT displays, *Displays*, **3**, 32 (1982).
26. Sine Patterns LLC 3800 Monroe Avenue Pittsford, NY 14534, USA.
27. P. Barten, Short course notes SC53: *MTF, CSF and SQRI for image quality analysis*, *IS&T/SPIE Symposium on Electronic Imaging: Science and Technology*, IS&T, Springfield, VA, 1997.
28. D. R. Lehmebeck and J. C. Urbach, Scanned Image Quality, In *Optical Scanning*, G. F. Marshall, Ed., Marcel Dekker, New York, 1991, chap. 3. p. 83–158.
29. Image Analyser SFR Plug-in User Guide, Internet publication: <http://www.pima.net/it10a.htm> (1998).
30. D. Williams, Benchmarking of the ISO 12233 Slanted-Edge Spatial Frequency Response Plug-in, *Proc. IS&T PICS Conference*, IS&T, Springfield, VA, 1998, p. 133, 1998.
31. P. D. Burns, Slanted-edge MTF for digital camera and scanner analysis, *Proc. IS&T PICS Conference*, IS&T, Springfield, VA, 2000, p. 135.
32. A. M. Ford, *Relationships Between Image Quality and Image Compression*, PhD Thesis, University of Westminster, UK, 1997, chap. 4. pp. 63–94.